Archives of Materials Science and Engineering

Volume 52
Issue 2
December 2011
Pages 101-111

International Scientific Journal
published monthly by the
World Academy of Materials
and Manufacturing Engineering

Basic properties of 3D cast skeleton structures

M. Cholewa*, T. Szuter, M. Dziuba
Foundry Department, Silesian University of Technology, ul. Towarowa 7, 44-100 Gliwice, Poland
* Corresponding author: E-mail address: miroslaw.cholewa@polsl.pl

Received 12.09.2011; published in revised form 01.12.2011

ABSTRACT

Purpose: of this paper is to present recent achievements in field of skeleton structures. The aim of this work is to show results of searching for mechanically and technologically advantageous micro- and macrostructures. Methods of microstructure controlling were described. Most important parameters of the manufacturing process were identified.

Design/methodology/approach: The influence of internal topology to stress distribution was described with the use of computer simulations. Simulations of the mold filling processes were also carried out. Real experiments were performed to prove the simulation results. The Qualitative and quantitative metallographic analysis were also carried out.

Findings: It was found that the octahedron shape of internal cell causes best stress distribution and that the skeleton castings are a good alternative for cellular materials such as metal foams, lattice structures and sandwich panels. Their structured arranged topology allows precise design of properties.

Research limitations/implications: Casting methods used to manufacture materials such as described skeleton castings confirmed their usefulness. Not well known and used yet rheological properties of liquid metals allow obtaining shape complicated structures near to metallic foams but structured arranged.

Practical implications: Technological parameters of the skeleton castings manufacturing process were developed. Without use of advanced techniques there is a possibility to manufacture cheap skeleton structures in a typical foundry. With use of advanced technology like 3D printing there are almost unlimited possibilities of the skeleton castings internal topologies.

Originality/value: Three dimensional cast skeleton structures with internal topology of octahedron confirmed their usefulness as elements used for energy dissipation. Obtaining the homogenous microstructure in the whole volume of complicated shape castings can be achieved.

Keywords: Skeleton casting; Metallic alloys; Porous materials; Aluminum casting; Simulation

Reference to this paper should be given in the following way:

M. Cholewa, T. Szuter, M. Dziuba, Basic properties of 3D cast skeleton structures, Archives of Materials Science and Engineering 52/2 (2011) 101-111.

MATERIALS MANUFACTURING AND PROCESSING

1. Introduction

Cellular structures (CS) like metallic foams, lattice structures or sandwich panels are designed as multifunctional structural elements. Their main properties are high strength with low weight, good resistance to dynamic loads, acoustic insulation and possibility of heat flow control. Properties of CS depend on material which these are made of and their internal features - topology and microstructure.

There are lot possibilities to produce these skeleton constructions and classic lattice structures. During designing

properties of these material structures three main factors should be taken into account:

- properties of the material which these are made of,
- topology of the structure - shape of internal cells, struts, ligaments,
- relative density of skeleton/foam as density of the structure to density of the material ratio.

Mechanical, thermal and electrical properties of CS are closely related to its application and manufacturing technique. Shape of internal cells, size of walls and ligaments are responsible for relative density. Micro- and macrostructure of presented skeleton castings are responsible for type of deformation of specific cells. This aspect is important due to deformation of the whole structure and its strength. Basic information was shown in Ashby's studies [1].

Constructions close to skeleton castings are made with different techniques. These constructions are manufactured with use of specific patterns, hollow tubes and rods. The cylinders are metallurgical bonded using brazing. The use of slightly bigger tubes instead of rods gives lower possibility of buckling with great lowering of mass [2].

CS can be manufactured with forging techniques (Fig. 1). The core is formed from steel plates with use of press. The core is bonded with outside walls with laser spot welding.

Those panels are resistant to dynamic loads and mainly used in aeronautics [3,4].

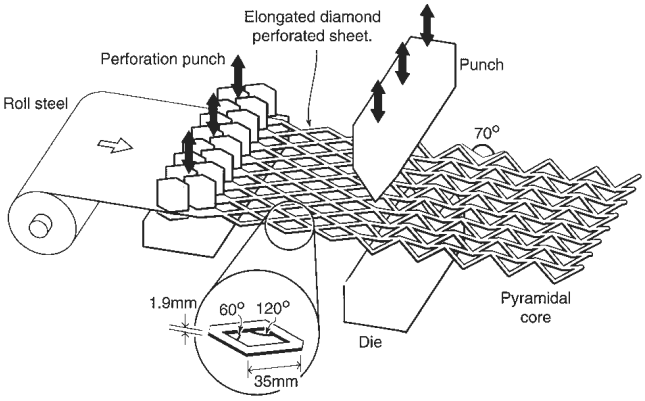

Fig. 1. Scheme of manufacturing of sandwich panels with pyramidal truss internal topology [3,4]

Foundry technologies are also used for manufacturing of lattice and skeleton structures. Traditional casting methods are applied. In this way without use of advanced techniques castings with different topology and wall thickness can be obtained [5].

Techniques of investment castings are also useful [6]. Together with the use of antigravity casting they provide possibility to obtain castings with ligaments of about 1.5 mm diameter [7]. This kind of castings are used by NASA for exhaust nozzle structures [8].

Casting techniques are used for manufacturing skeleton constructions where the core is made of cast AlSi tubes. It is less liable to buckling than skeleton castings, but manufacturing process is much more complicated. Each strut has to be mold and cast separately and then bonded together with welding technique [5,9].

Combination of electro-erosion and casting technology is also used. Skeleton constructions (Fig. 2) with pyramidal core are obtained this way [10].

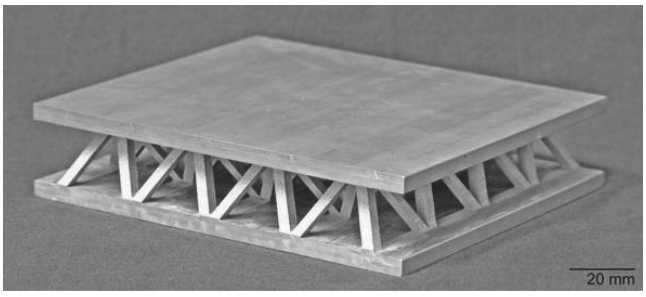

Fig. 2 Skeleton construction manufactured with casting and electro-erosion techniques [10]

Foundry techniques (molding, core making) put some limitation to the internal topology of skeleton castings. There is a limited number of macrostructures possible to mould. This problem can be solved by using additive methods of production.

Figure 3 is showing a model of skeleton casting made with 3D printing technology.

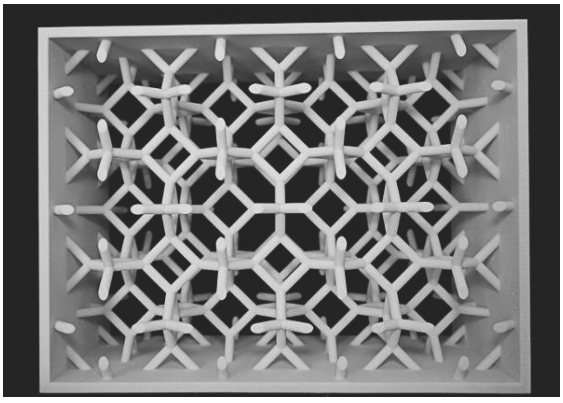

Fig. 3. Skeleton casting model made with 3D printing

Lattice/skeleton structures are also made from composites for example carbon fibers with hot preform moulding techniques. Obtained panels have compressive strength of about 40 MPa [11].

This types of constructions confirmed suitability as kinetic energy or blast absorbers. It is significant that only slight deformation of back panel was observed [3,13]. With change of density gradient in direction of force, it is possible to control quantity and kind of absorbed energy.

Moreover CS with open cells such as skeleton castings allows significant improvement of heat dissipation [14]. This makes possibility of using it as industrial power supplies heat radiators. Casings of power supplies made this way act also as part of heat dissipation system.

Potentially very wide possibilities of practical application of CS are a very important reason to its development also with the use of casting techniques. An additional reason is the beneficial rheological properties of liquid alloys which are not used entirely.

2. Description of studies

The aim of this work is to show results of searching for mechanically and technologically advantageous micro- and macrostructures. Alternative casting manufacturing techniques were also taken into account. The mechanical properties were analyzed by the use of numerical simulation. Simulations were used also to prove that the casting techniques are suitable for skeleton castings production with assumed internal topology. An important assumption while designing internal topology of skeleton castings is the possibility of manufacturing them with use of basic casting technologies without expensive equipment and laboratory precision.

The simulation investigation of mechanical deformation was performed in Ansys environment. For the purpose of the research three basic shapes of elementary cells were predestined. It was a cube, an octahedron and a truncated octahedron. Those types of elementary cells were chosen because of their perfect fulfillment of space. Additionally, those shapes allow to maintain symmetry in all three axles. This assumption is to preserve isotropy of mechanical properties in function of the topology. This solution gives basic predictions of skeleton castings properties and basic interpretations of dynamic deformation depending on the point and direction of the force vector.

Recently in the Foundry Department of the Silesian University of Technology a few variations of skeleton casting manufacturing techniques were developed. Skeleton castings are made from cast iron, steel and aluminum alloys. Some of them are shown in this article. The technological geometry of skeleton model was developed (Fig. 3). Single cell of internal topology is a truncated octahedron so called Kelvin's octahedron. Polymer model was used to make a ceramic core of the mold.

Technological parameters for skeleton casting microstructure control were investigated. Methods of obtaining homogeneous microstructural features in whole volume of castings were developed.

2.1. Simulations

For preparing of the 3D model and carrying out necessary simulations Ansys software was used. Ideally plastic model was used. Force was perpendicular and focused to point in geometric center of the biggest wall.

In Figures 4-6 the analyzed geometry and results of early analysis of deformation in each case were shown. Figure 4 shows the standard topology based on a cube. Distribution of deformation shows that the rods parallel to the force were the most deformed. The main part of the force is compressive so it determines high possibility of negative buckling. Moreover, most of the rods do not participate in stress distribution, so this topology is ineffective.

In Figure 5 next internal topology of skeleton casting was showed. Rods of this lattice form an octahedron. Perpendicular force works on rods at an angle of 45°. This causes advantageous in the distribution of force in the early deformation involving reactions of a higher number of rods. Most of the rods were deformed. In this case the dominating force is no longer compressive. Octahedron meets Maxwell's criterion of stability. This criterion gives a possibility to design material in which stretching forces will be dominating [1,14].

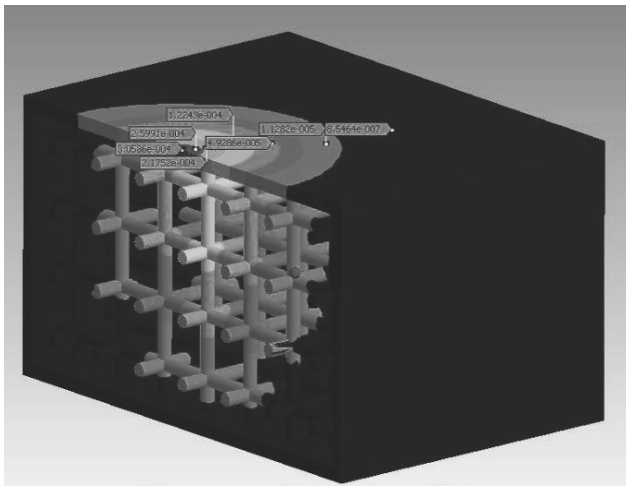

Fig. 4. Results of simulation. Distribution of strain as response to load in whole volume. Cube elementary cells. Axial cross-section

Last considered topology was based on truncated octahedron. This expanded geometry allows to good load transfer in whole volume of skeleton casting. Also, like in octahedron case, force works on rods at an angle of 45°. Maximum structural deformation was observed. It suggests that this topology of skeleton casting as the best for energy absorbing. Polygon truncated octahedron does not meet Maxwell's criterion. Skeleton castings with the topology based on truncated octahedron are bending dominating structures.

The main aim is minimization of buckling with possible most share of stretching forces.

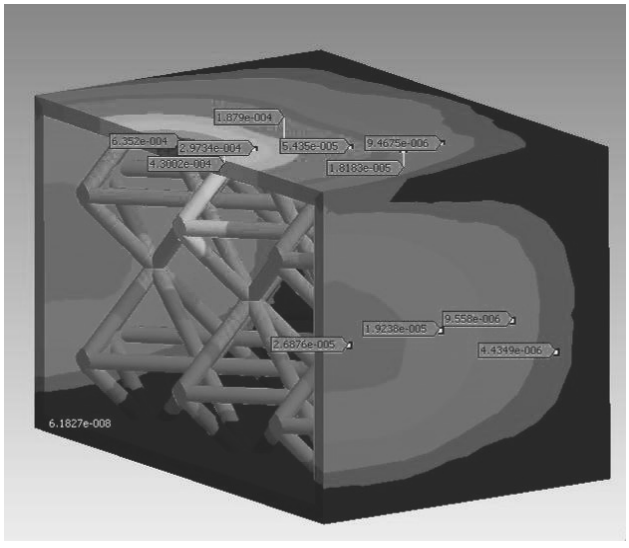

Fig. 5. Results of simulation. Distribution of strain as response to load in whole volume. Octahedron elementary cells. Axial cross-section

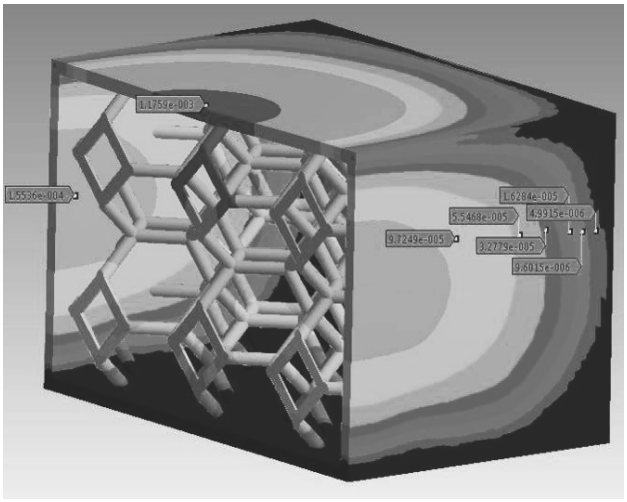

Fig. 6. Results of simulation. Distribution of strain as response to load in whole volume. Truncated octahedron elementary cells. Axial cross-section

2.2. Simulations of casting processes

Mold filling simulation was used to ensure good filling of the complicated skeleton casting geometry, also to investigate temperature distribution in the casting and mold. Solidification process was analyzed as well. In presented case, liquid metal flows first to outside walls of the casting and next it fills the internal channels of core until complete filling of the mold cavities. Figure 7 shows volume fraction of liquid phase during mold filling.

Carried out simulations confirmed good filling of mold cavities. Gating system was also confirmed as best for good feeding of such complicated casting geometry. Simulations allowed describing the regions with disturbed heat dissipation and the latest solidification areas. Depending on casting process parameters after modification of thermal properties of mold, technological confidence of microstructure of skeleton casting was achieved [15].

2.3. Manufacturing of test castings

Manufacturing of skeleton castings cores

One of the basic and most important problems in technology of skeleton castings is the core making. The core is responsible for the final shape of cells of skeleton castings. The aim is to create a core with the properties allowing multifunctional use. On one hand, like an element which is reproducing the internal surface, and on the other hand with necessary additions the core will be raising mechanical properties of the whole skeleton construction. Especially the properties of energy absorption in the whole volume of structure.

a)

b)

c)

d)

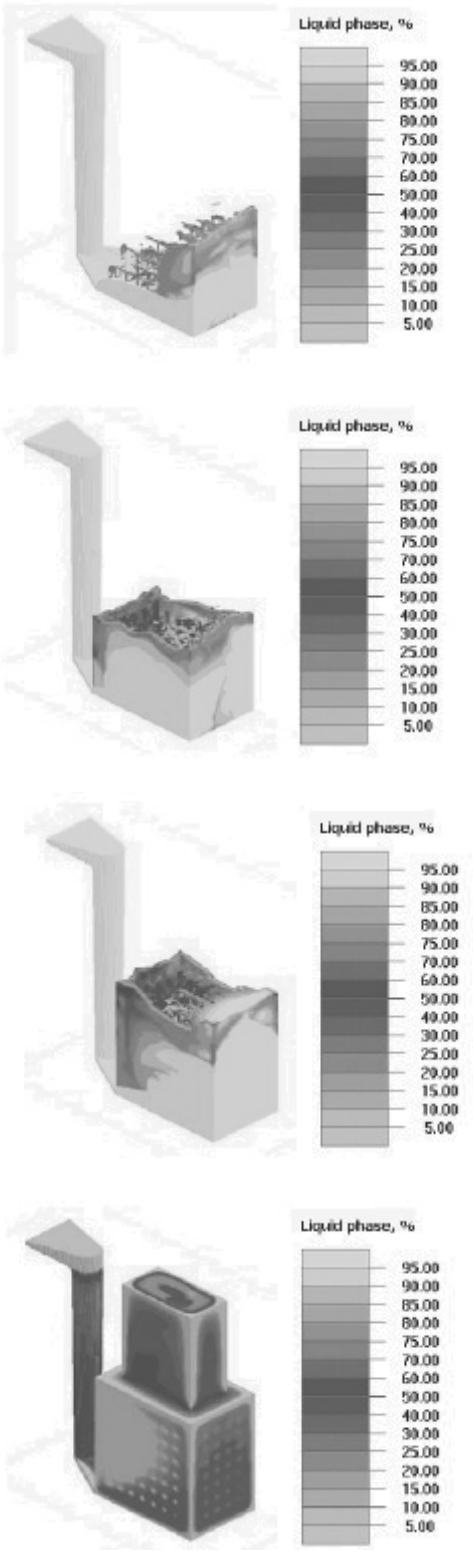

Fig. 7. Volume fraction of liquid phase during mold filling

Among technologies developed in the Foundry Department of the Silesian University of Technology there is one considering manufacturing of layers and semi layers of core with the use elastic or rigid core boxes.

Another concept is based on manufacturing core in rigid core box and puncturing the holes. Those holes are creating a web of rods and struts of internal topology of skeleton casting.

To manufacture cores typical core materials are being used. Low conductivity, ceramic, aluminosilicate, porous materials showed on Figure 8.

The way to manufacture cores of skeleton castings is related with type of material which these are made of. Cores of skeleton castings can be made with cristobalite matrix. Use of gypsum as core material allows easy removing of the core after casting. Use of ceramic bricks (Fig. 8) allows obtaining high strength cores with complicated geometry. This type of cores is very adhesive to the casting surface.

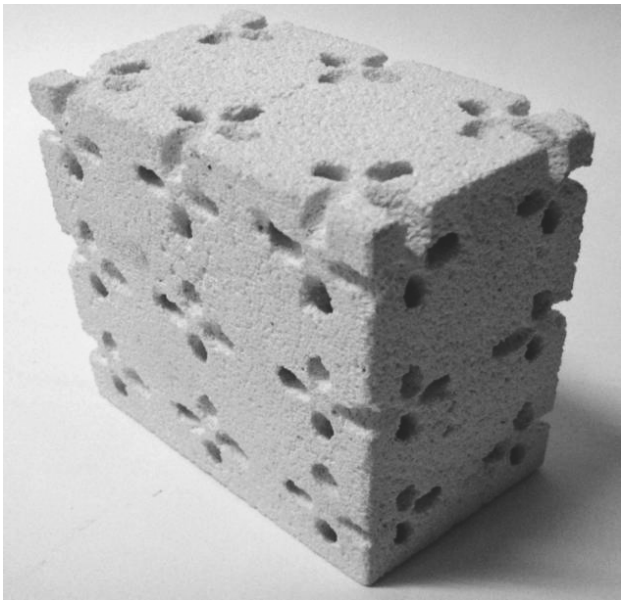

Fig. 8. Ceramic, porous aluminosilicate core

One of the alternatives is mass with alominosilicate microspheres. The adventage of use of bentonite as a binder mass is its easy removal from casting (Fig. 9). There is one common parametry of all types of masses used in skeleton castinge - high thermal insluating.

Casting process parameters

Skeleton castings are sand molded. Only way to obatain good quality casting was selecting a proper gating system. No additional assisting in mold filing was used. Castings were made from neareutectic AlSi alloy and from pure aluminium. The chemical composition of the used alloy is shown in Table 1.

This alloys crystallizes forming fine grained structures. AlSi11 alloy is recommended for obtaining casts of complicated shapes.

Table 1.
The chemical constitution of AlSi11

Eleme.	Al	Si	Mg	Mn	Cu	Ni	Zn	Sn
Comp. %	82.9	10.5	0.1	0.5	2.5	0.3	3.0	0.15

Antimony was used to improve the castability of the alloy. Antimony gives very high castability to the alloys without gassing it. The addition of Sb in the amount of 0.4% mass was applied.

In presented research antymony was applied in order to decrease surface tension of liquid alloy, to minimize production of Al_2O_3 oxides on front of the stream and to maximize the castability of the alloy.

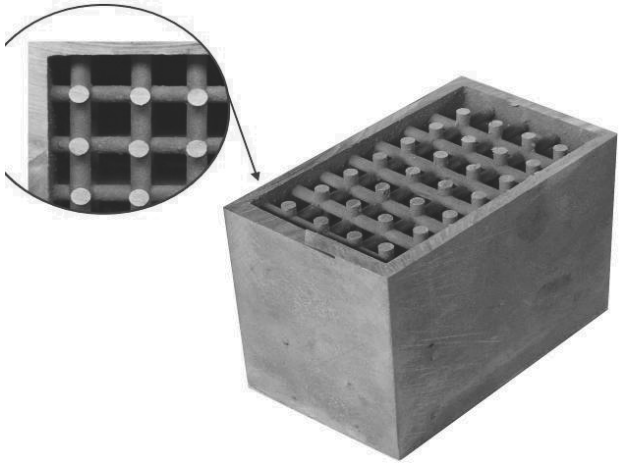

Fig. 9. Skeleton casting cross section after removing the core

2.4. Microstructure steering

Homogenus microstructute in whole volume of casting is as important as the type of material and internal topology.

Steering of microstructure was realized by:

- selection of casting alloy, which provides the required castability and filling of volume of skeleton castings,
- using of heat-insulating core materials, which provides uniformly filling of volume of skeleton castings,
- using variable technological conditions manufacturing of skeleton castings.

The study was performed as a function of pouring temperature, temperature of the mould and height of the gating system. The studies used:

- three-level experiment plan. Then microstructural studies were performed:
- qualitative analysis of metallographic specimens,
- quantitative analysis of crystals of eutectic silicon in skeleton castings,
- analysis of the dendrite arm spacing (DAS) of the α solution.

Example of closed aluminum skeleton casting and typical regions of casting in which authors compared microstructure were shown in Figure 10.

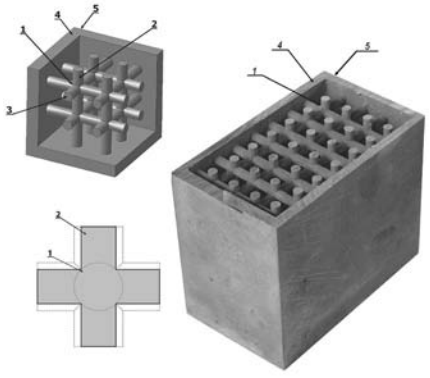

Fig. 10. Typical regions in which author compared microstructure: 1 - skeleton node corner; 2 - longitudinal section; 3 - cross-section; 4 - central elements of corner wall which closed the skeleton; 5 - external surface of corner wall which closed the skeleton [1,2]

Structural constituent of alloy is: solution α of silicon in aluminum and crystals of eutectic (α + Si) silicon in interdendritic regions. Microstructures particular elements of consecutive skeleton casting were shown in Figure 11. Numerical designations in the right upper corner meet a description in Figure 10. Sequence of micrograph meet the increase of dimension of structural constituent.

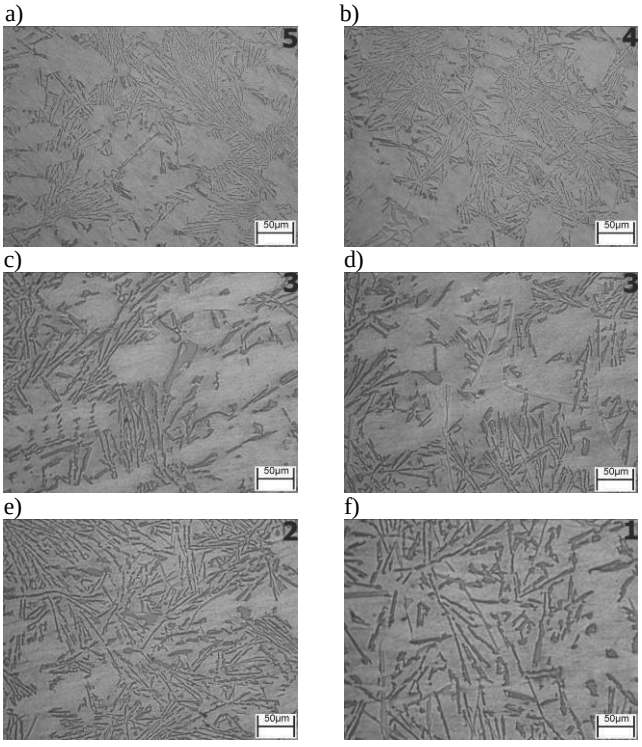

Fig. 11. Microstructures particular elements of skeleton casting (AlSi11, T_{pour} 953 K, T_{mould} 293 K, h - 300 mm): a- external surface of wall which closed the skeleton, b- central elements of wall which closed the skeleton, c, d, - longitudinal section of skeleton connector, e- cross-section of skeleton connector, f - corner of node, designation numerical (1-5) meet a description in Fig. 14

In microstructure pictures the MultiScanBase software has automatically found silicon crystals. Stereological parameters for every silicon crystals were measured.

Maximal and minimal and average values of stereological parameters for all analyzed regions were determined. On basis of values of stereological parameters refinement degree was determined. Values of stereological parameters for selected sample were shown in Table 2. (B/L) and (P/A) factors and *Na* parameter were determined. *Na* parameter determines silicon crystals number on 1 mm^2 surface.

Then, the results of analysis were presented by charts - histograms $N_A = f(A)$ silicon crystals number in surface area classes of silicon crystals for extreme regions of example skeleton casting (Fig. 12).

Table 2.
Values of measured and calculated stereological parameters of silicon crystals for researched regions of consecutive castings - sample 5 (AlSi11, T_{pour} 1013 K, T_{mould} 333 K, h - 265 mm)

Region	A [µm²]	L [µm]	B [µm]	P [µm]	$\frac{B}{L}\left[\frac{1}{1}\right]$	$\frac{P}{A}\left[\frac{1}{\mu m}\right]$
Aver.	**35.70**	**31.33**	**15.21**	**10.92**	**0.50**	**0.47**
Max	3794.74	559.54	315.33	680.36	0.95	1.20
Min	3.64	7.04	1.71	0.40	0.05	0.09
Aver.	**28.77**	**29.44**	**14.79**	**9.98**	**0.52**	**0.47**
Max	961.44	377.85	204.94	299.41	1.00	1.19
Min	3.71	7.29	1.71	1.93	0.10	0.14
Aver.	**23.31**	**25.07**	**12.43**	**8.64**	**0.50**	**0.52**
Max	1788.55	350.72	260.76	344.61	0.96	1.29
Min	1.02	3.08	0.85	0.67	0.06	0.18
Aver.	**28.96**	**27.75**	**13.73**	**9.56**	**0.51**	**0.49**
Max	1735.61	483.33	162.71	451.50	0.97	1.14
Min	3.64	7.04	1.71	1.91	0.06	0.11
Aver.	**19.61**	**26.10**	**11.08**	**7.99**	**0.45**	**0.54**
Max	920.74	252.15	171.65	220.84	0.96	1.23
Min	3.71	7.29	1.21	0.48	0.07	0.02

Presented empirical distributions N_A for research regions was approximated by function (Fig. 13):

$$F(A) = \frac{U \cdot Z \cdot \exp[Z \cdot (W - \log(A))]}{[1 + \exp(Z \cdot (W - \log(A)))]^2} \quad (1)$$

where:
A - area of crystal skeleton castings [μm^2];
U - index of fraction summary volume of silicon crystals [%];
W - average logarithmic surface area of silicone crystals [μm^2];
Z - index of diversification of surface of silicone crystals [$1/\mu m^2$] (the Z value is greater - distribution curve is a "slimmer").

Figure 13 shows examples of approximate relation between objects quantity (y=F(x)) and A logarithm (log x) for regions of skeleton castings with different pouring temperature and temperature of mold. In Table 3 parameters of function, which approximate of distributions of Area A for regions of skeleton castings were shown.

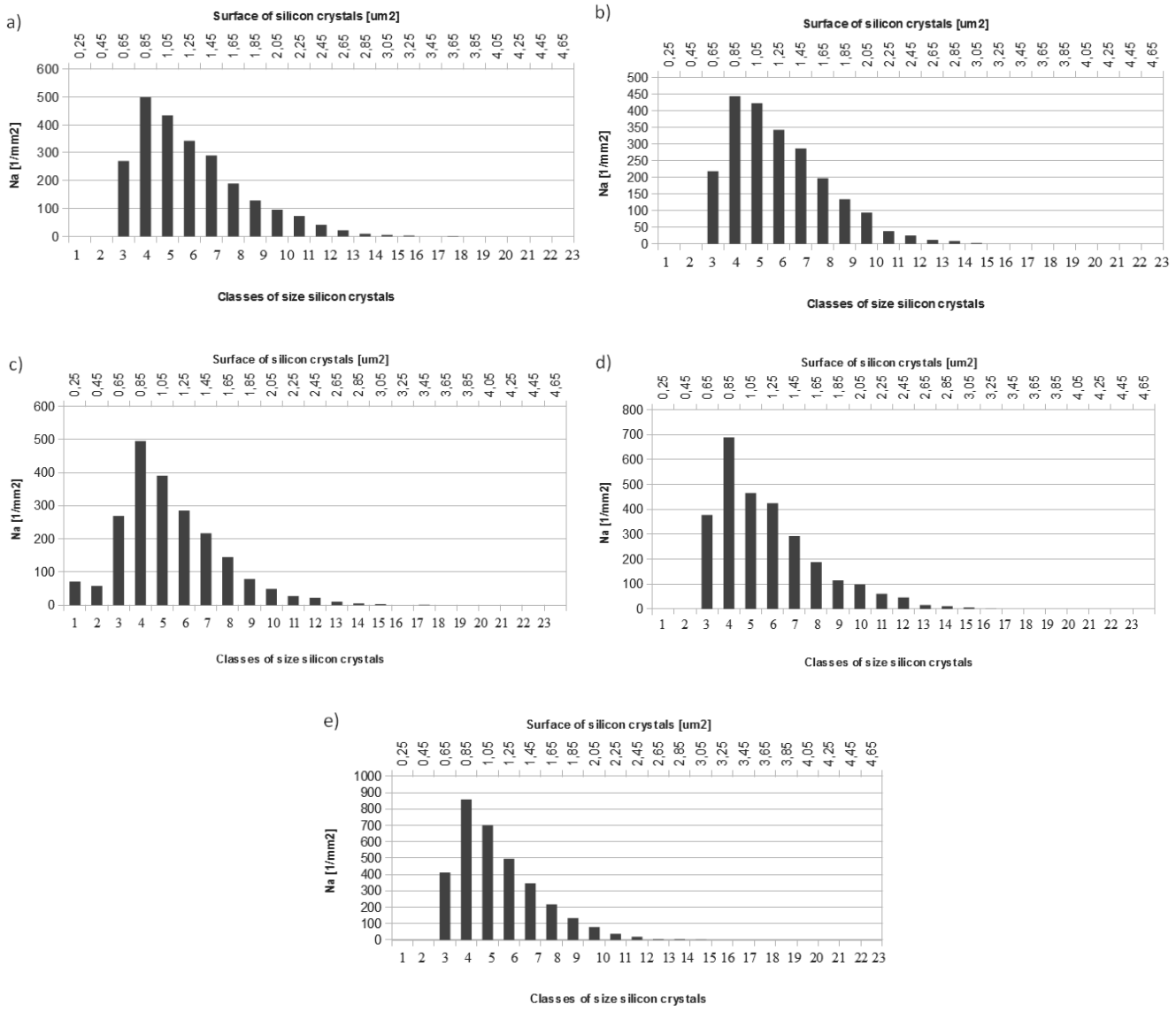

Fig. 12. Quantities Na of silicon crystals in classes of size their the surface (AlSi11, T_{pour} 1013 K, T_{mould} 333 K, h - 265 mm for research regions of castings: a) region 1; b) region 2; c) region 3; d) region 4; e) region 5

Dendrite arm spacing of α solution was determined. Samples were grinded and polished and then etched in 20% NaOH water solution. Results of dendrite arm sparing for samples from experiment plan are shown in Table 2 (Numerical designations meet a description in Fig. 10).

Dendrite arm spacing in typical and extreme regions 1 and 5 was investigated. For regions 1 and 5 will provide the greatest diversification of DAS which connected with different cooling rate in these regions. The great scatter of results in regions 1 and 5 for castings 3, 4 and 7 was observed. Distributions of secondary dendrite-arm spacing diagrams for sample 5 were presented in Figure 14.

Table 3.
Parameters function, which approximate of N_A distributions for regions of skeleton casting (T_{pour} 1013 K, T_{mould} 333 K, h - 265 mm)

Region of casting	Function, which approximate of N_A distribution				
	Measured parameters function			Statistical parameters	
	U [%]	W [um^2]	Z [1/mm^2]	correlation	Fisher's test
1	507	1.07	3.9	0.94	14.8
2	692.51	1.09	3.01	0.79	3.85
3	637.26	0.96	3.10	0.82	4.59
4	777.4	1.00	4.35	0.84	4.58
5	1029.2	0.99	4.28	0.78	3.46

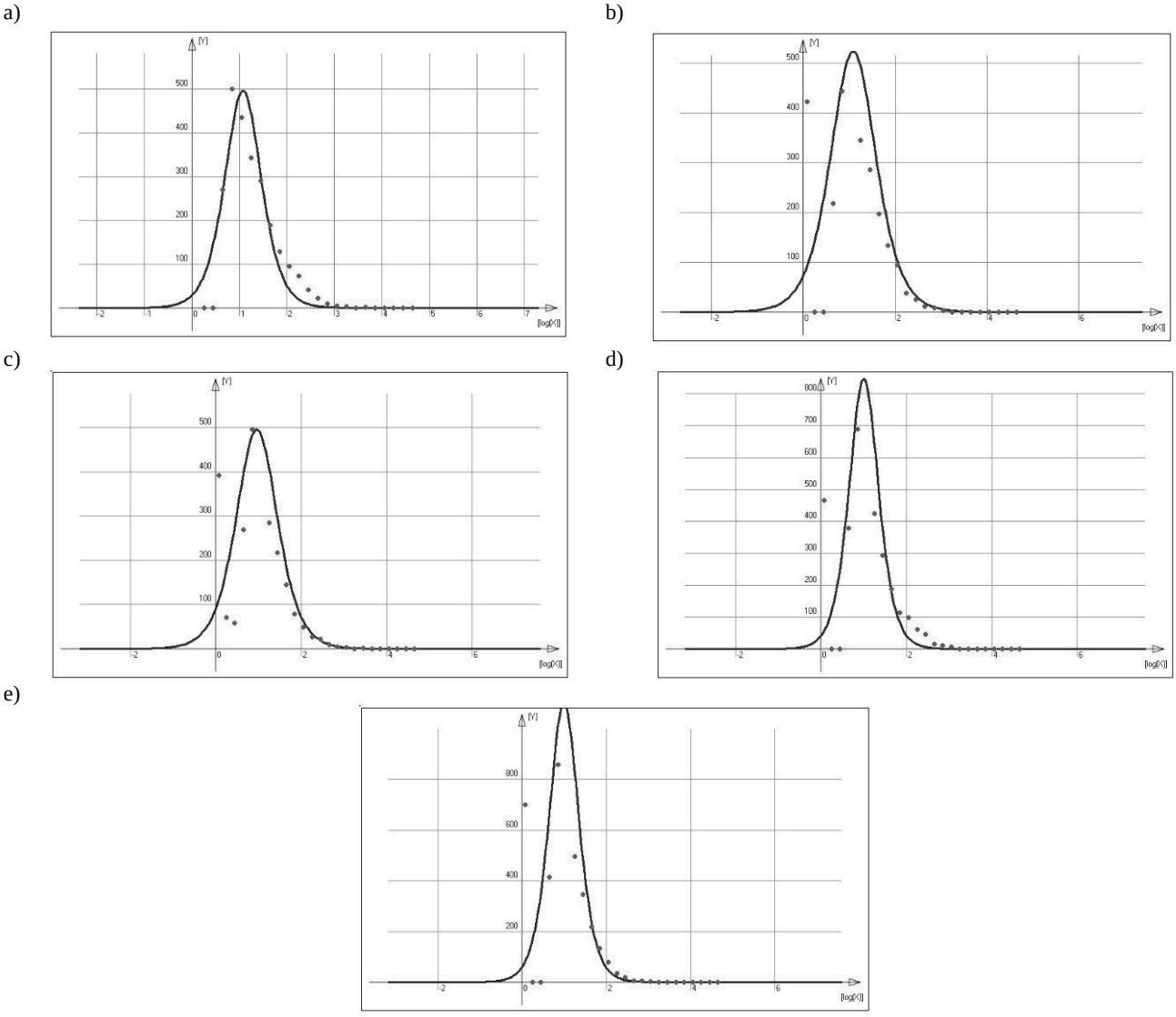

Fig. 13. Functional, approximation size of objects [1/1] related to logarithm of measured A [μm2] for regions of skeleton castings which manufactured on conditions T_{pour} 1013 K, T_{mould} 333 K, h - 265 mm: a) region 1, b) region 2, c) region 3, d) region 4, e) region 5

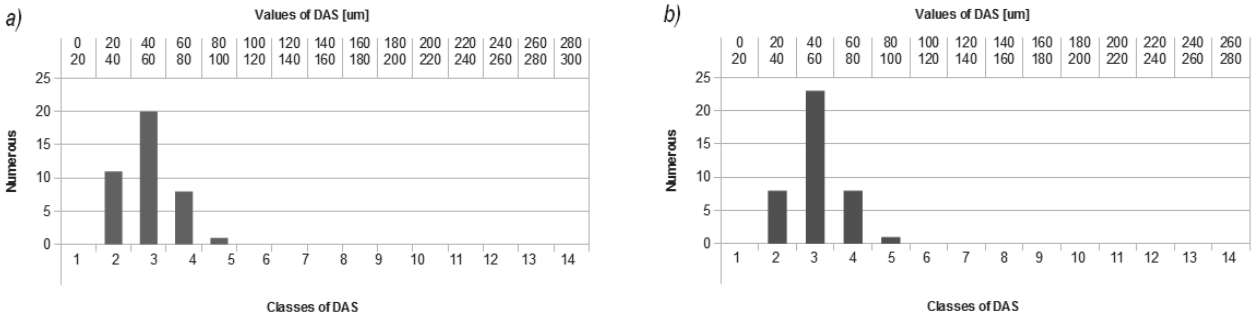

Fig. 14. Distribution of secondary dendrite-arm spacing for selected regions of casting - sample 5 (AlSi11, T_{pour} 1013 K, T_{mould} 333 K, h - 265 mm)

During crystallization different conditions of heat dissipation occurred. Structure of sections element connector of skeleton (Fig. 1 a, b point 2, 3) and in corner of a node (Fig. 1 a point 1) and on wall which closed the skeleton (Fig. 1 c point 4, 5) were compared.

The highest averages of surface of silicon crystals is in the region 1 (Table 2), which confirmed that the least refinement of skeleton casting structure was on the corner of node. The lowest average of surface of silicon crystals is in the region 5 for all skeleton castings, which connected with occurrence the most refined eutectic silicon and rapid heat dissipation.

Empirical analysis of distributions $N_A=f(A)$ was shown, that the most of silicon crystals in the highest classes their surface were in skeleton node corner which is confirmation of lowest refinement. With rising of classes of silicone crystals there is lowering of their quantity. In the highest classes of size there are no silicon crystals. The most of silicon crystals in lowest classes of size of their surface in external surface of wall which are closing all of the skeleton castings. This is confirmation of greatest refinement.

B/L factor (Table 2) determines degree of extension of silicon crystals. The lower value of factor the more elongated silicon crystals are. Values of B/L factor are similar for all analyzed regions each researched skeleton castings. Whereas P/A factor determine surface development of silicon crystals. For all analyzed regions P/A factor the greatest values is in region 5, next in region 4, which connected with rapidly heat give up occurred in this regions.

The graphic of the approximated function $N_A(A)$ and the value of the parameter U ,W and Z (Table 3, Fig. 4) were show that summary indicator of the volume fraction of silicon crystals reaches a high value. Logarithmic area of silicon crystals is low. This demonstrates the presence in the structure of the skeleton castings a large number of small silicon crystals.

The least averages dendrite arm spacing (Table 4) for castings for which in four regions authors investigated the research is for castings 4 and 7 in regions 5. The greatest averages values of DAS are for casting 3 in region 1.

The graphic of the approximated function NA(A) and the value of the parameter U and W were show that summary indicator of the volume fraction of silicon crystals reaches a high value. Logarithmic area of silicon crystals is low. This demonstrates the presence in the structure of the skeleton castings a large number of small silicon crystals.

For castings 1, 5, 6, 8, 9, 10, 11 for which average DAS was measured in specific extreme regions research provide numerical description of cooling rate influence on refinement degree of structure. The least averages dendrite arm spacing for castings 9 and 11 are in region 5. For castings 1, 5, 6, 8, 10 dendrite arms spacing the least values are in region 1. Values DAS in region 1 and 5 for this castings achieves are similar (Table 4).

The least averages dendrite arm spacing (Table 4) for castings for which in four regions authors investigated the research is for castings 4 and 7 in regions 5. The greatest averages values of DAS are for casting 3 in region 1.

Values DAS in region 1 and 5 for this castings achieves are similar (Table 3).

Table 4.
Dendrite arm spacing for select regions of skeleton castings

Sample	Measure range	Dendrite arm spacing [μm]			
		min	max	average	stand. dev.
1 T_{pour} 1013 K, T_{mould} 373 K, h - 300 mm	region 1	19.11	86.53	47.64	15.89
	region 5	19.11	86.65	51.60	15.36
3 T_{pour} 953 K, T_{mould} 373 K, h - 230 mm	region 1	120	350	188	67
	region 5	70.01	240	145.11	38
4 T_{pour} 953 K, T_{mould} 293 K, h - 300 mm	region 1	60.02	202	118	34
	region 5	78.73	118.7	96.62	11.69
5 T_{pour} 1013 K, T_{formy} 333 K, h - 265 mm	region 1	26.27	82.20	49.14	12.86
	region 5	22.52	86.06	50.28	13.88
6 T_{pour} 953 K, T_{mould} 333 K, h - 265 mm	region 1	13.51	95.57	44.10	17.40
	region 5	22.52	95.02	59.77	20.95
7 T_{pour} 983 K, T_{mould} 373 K, h - 265 mm	region 1	71.10	212.0	123	29
	region 5	71.20	173.3	117.02	25
8 T_{pour} 983 K, T_{mould} 293 K, h - 265 mm	region 1	22.97	82.20	52.26	14.94
	region 5	24.26	93.73	52.68	15.49
9 T_{pour} 983 K, T_{mould} 333 K, h -300 mm	region 1	16.24	96.40	53.31	20.36
	region 5	14.24	84.15	48.96	15.49
10 T_{pour} 983 K, T_{mould} 333 K, h - 230 mm	region 1	16.24	81.21	38.98	12.26
	region 5	20.14	91.87	49.40	16.16
11 T_{pour} 983 K, T_{mould} 333 K, h - 265 mm	region 1	16.24	85.47	51.37	16.61
	region 5	22.52	90.20	48.04	16.57

On basis of results of microstructural analysis authors compares research of samples (Table 5). The aim of analysis was selected samples on least diversification of refinement degree of structure and least silicon crystals.

The least average overall surface of silicon crystals is for sample 5 (A_{avg} = 27.27 [μm^2]). B/L factor highest values is for sample 5, factor value is from 0.45 to 0.52 for extreme regions of skeleton castings, this is connected with least elongated silicon crystals in this sample.

Values of P/A factor for sample 5 are variables in range least in extreme regions. Values of factor are from 0.47 to 0.54. The least values of dendrite arm spacing are for samples 1, 5, 6, 9, 10. Authors selected samples 5 for which DAS are variables in range limit and DAS values are the least for extreme regions of casting.

On basis research authors state that the best structural properties for samples 5 (AlSi11, T_{pour} 1013 K, T_{mould} 333 K, h - 265 mm).

Table 5.
Results of structural analysis [2]

No. of casting	$\frac{B}{L}\left[\frac{1}{1}\right]$	$\frac{P}{A}\left[\frac{1}{\mu m}\right]$	DAS [μm]
1	0.42 - 0.51	0.47 - 0.60	47.6 - 51.6
2	0.44 - 0.48	0.44 - 0.54	54.1 - 69.7
3	0.41 - 0.46	0.81 - 9.33	116.2 - 188
4	0.31 - 0.45	0.83 - 0.99	96.6 - 120
5	0.45 - 0.52	0.47 - 0.54	49.1 - 50.2
6	0.39 - 0.44	0.48 - 0.56	44.1 - 59.7
7	0.40 - 0.52	1.07 - 12.27	117 - 164
8	0.45 - 0.51	0.48 - 0.56	52.2 - 52.6
9	0.39 - 0.43	0.47 - 0.56	49 - 53.3
10	0.44 - 0.46	0.47 - 0.55	39 - 49
11	0.40 - 0.48	0.50 - 0.55	48 - 51.3

3. Conclusions

Technological parameters of the skeleton castings manufacturing process were developed. The mechanical simulations allowed to show the most interesting internal topologies of the skeleton castings according to the mechanical properties.

Firstly based on simulation of casting process then on real experiments optimal parameters like type and temperature of liquid alloy, type of gating system, type of molding materials and mold temperature were described. Core materials were developed. The need of high thermal insulating and good strength has met alumionsilicate bricks. Technology of manufacturing of skeleton castings cores was developed with taking into account foundry conditions of manufacturing.

Based on research the possibility to control the structure by alloy choice which providing the required alloy castability was confirmed. The addition of antimony as a modifier increased the melt castability and consequently, increased the degree of filling of the skeleton castings made in technological conditions selected according to the Hartley's plan experiment.

The choice of insulating material for the core of skeleton castings has also a significant impact on their structural properties.

Skeleton castings are good alternative for cellular materials such as metal foams, lattice structures and sandwich panels. Their structured arranged topology allows precise design of properties. Casting methods used to manufacture materials such as described skeleton castings confirmed their usefulness. Not well known and used yet rheological properties of liquid metals allow obtaining shape complicated structures near to metallic foams but structured arranged.

Fig. 15 shows model of Ashby's ideal metallic foam [1]. It was made with additive methods of manufacturing - 3D printing. It will be used for making core and in consequence ready casting of ideal metallic foam.

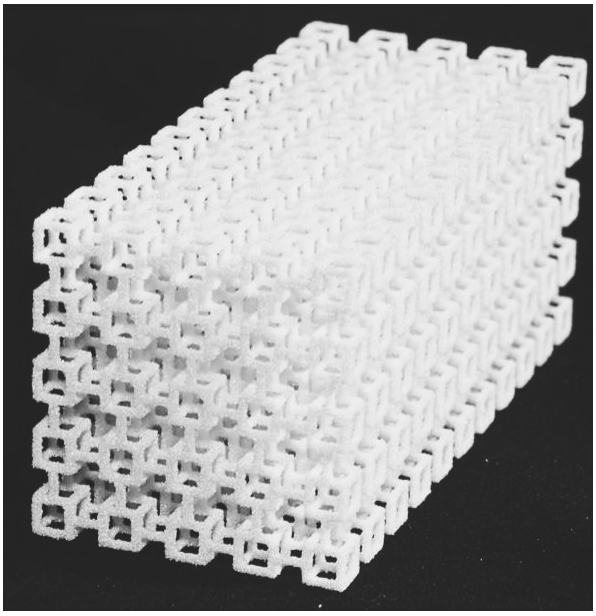

Fig. 15. 3D printed model of Ashby's ideal foam

References

[1] M.F. Ashby, The properties of foams and lattices, Philosophical Transactions Of The Royal Society A - Mathematical Physical And Engineering Sciences 364 (2006) 15-30.

[2] D.T. Queheillalt, H.N.G. Wadley, Cellular metal lattices with hollow trusses, Acta Materialia 53 (2005) 303-313.

[3] K.P. Dharmasena, H.N.G. Wadley, K. Williams, Z. Xue, J.W. Hutchinson, Response of metallic pyramidal lattice core sandwich panels to high intensity impulsive loading in air, International Journal of Impact Engineering 38 (2011) 275-289.

[4] G.W. Kooistra, V.S. Deshpande, H.N.G. Wadley, Compressive behavior of age hardenable tetrahedral lattice truss structures made from aluminum, Acta Materialia 52 (2004) 4229-4237.

[5] M. Cholewa, T. Szuter, Geometrical and mechanical analysis of 3D casted skeleton structures, Archives of Foundry Engineering 10/2 (2010) 23-27.

[6] J.C. Wallach, L.J. Gibson, Mechanical behavior of a three-dimensional truss material, International Journal of Solids and Structures 38 (2008) 7181-7196.

[7] M.G. Hebsur processing of in-718 lattice block castings, Proceedings of the 131st Annual Meeting and Exhibition sponsored by The Minerals, Metals, and Materials Society.

[8] V.V. Vasiliev, A.F. Razin, Anisogrid composite lattice structures for spacecraft and aircraft applications, Composite Structures 76 (2006) 182-189.

[9] J. Xiong, L. Maa, L. Wua, M. Li, A. Vaziri, Mechanical behavior of sandwich panels with hollow Al-Si tubes core construction, Materials and Design, 2010.

[10] D.T. Queheillalt, Y. Murtyb, H.N.G. Wadley, Mechanical properties of an extruded pyramidal lattice truss sandwich structure, Scripta Materialia 58 (2008) 76-79.
[11] M. Li, L. Wu, L. Ma, B. Wang, Z.Guan, Mechanical response of all-composite pyramidal lattice truss core sandwich structures, Journal of Materials Sciences and Technology 27/6 (2011) 570-576.
[12] V.S. Deshpande, N.A. Fleck, One-dimensional response of sandwich plates to underwater shock loading, Journal of the Mechanics and Physics of Solids 53 (2005) 2347-2383.
[13] T.J. Lu, L. Valdevit, A.G. Evans, Active cooling by metallic sandwich structures with periodic cores, Progress in Materials Science 50 (2005) 789-815.
[14] V.S. Deshpande**,** M.F. Ashby, N.A. Fleck**,** Foam topology: bending versus stretching dominated architectures, Acta Materialia 49 (2001) 1035-1040.
[15] M. Cholewa, M. Dziuba-Kałuża, Numerical simulation of pouring and solidification of closed skeleton casting, Archives of Foundry Engineering 8/3 (2008) 9-12.